

Circularly photostimulated electrogyration in europium- and terbium-doped GaN nanocrystals embedded in a silica xerogel matrix

This article has been downloaded from IOPscience. Please scroll down to see the full text article.

2005 J. Phys.: Condens. Matter 17 5235

(<http://iopscience.iop.org/0953-8984/17/34/008>)

View [the table of contents for this issue](#), or go to the [journal homepage](#) for more

Download details:

IP Address: 129.252.86.83

The article was downloaded on 28/05/2010 at 05:52

Please note that [terms and conditions apply](#).

Circularly photostimulated electrogyration in europium- and terbium-doped GaN nanocrystals embedded in a silica xerogel matrix

I V Kityk¹, M Nyk², W Strek³, J M Jablonski³ and J Misiewicz²

¹ Institute of Physics, J Długoż University of Częstochowa, Częstochowa, Poland

² Institute of Physics, Technical University of Wrocław, Wrocław, Poland

³ Institute of Low Temperature and Structure Research, Polish Academy of Science, Wrocław, Poland

E-mail: i.kityk@ajd.czyst.pl

Received 6 February 2005, in final form 20 June 2005

Published 12 August 2005

Online at stacks.iop.org/JPhysCM/17/5235

Abstract

Circularly polarized optical poling was proposed and discovered for GaN nanocrystallites embedded in a silica xerogel matrix. The method consists of the creation of screw-like polarization of the medium during the interaction of two circularly polarized coherent bicolour beams. It was shown that doping of the GaN nanocrystallites by Tb³⁺ and Eu³⁺ ions leads to substantial enhancement of the electrogyration. The effect observed is a consequence of the superposition of nanoconfined effects and the contribution of the localized rare-earth 4f levels. The role of the anharmonic electron–phonon interaction is discussed. The photoluminescence and cathodoluminescence spectra of the GaN composites were investigated. It was demonstrated that the Eu-doped nanocrystallites give a substantially higher effect of the electrogyration compared to the Tb-doped and non-doped ones.

(Some figures in this article are in colour only in the electronic version)

1. Introduction

Optical poling has substantial advantages compared to electric-field or corona poling, consisting of the creation of the required symmetry in the medium without the necessity of using electrodes, particularly in materials with high conductivity. Nanocrystallites (NCs) of semiconductors doped by rare earths present particular interest for the electrogyration (EG), which consists of the optical activity induced by an external electric field.

An appearance of optical activity linearly dependent on the electric field (EG) was theoretically predicted by Zheludev [1] for crystals using phenomenological symmetry considerations. The effect may be linear or quadratic with respect to applied electric field

and may be described by third- or fourth-rank axial tensors, respectively. The linear effect is called linear EG and is described by axial third-rank axially symmetric tensors. In contrast to the linear electrooptics (Pockels) effect, it can be observed in non-centrosymmetric as well as in centrosymmetric condensed matters. Experimentally this effect was first discovered by Vlokh [2]. The first observed effect was a quadratic one with respect to the applied electric field vector. The linear EG described by third-rank axial tensors was also discovered by Vlokh *et al* [3, 4]. All these effects were observed in single crystals and the values of the EG coefficients were relatively low (not more than a few degrees per cm). This factor restrained the application of the effect in optical telecommunication and quantum electronic devices. In order to find materials with enhanced EG strength the effect was explored in ferroic materials [5], aluminium samples [6] and photorefractive materials [7].

Phenomenologically the EG is described by

$$\rho = \gamma_{ijk} E_j^{(0)} E_k^{(\omega)}, \quad (1)$$

where ρ is the rotational strength at a fixed external electric field strength $E_j^{(0)}$; γ_{ijk} is an axial third-rank tensor with the direction of applied electric field along the j direction and the polarization of incident light along the k direction. j indicates the direction of light propagation.

A simple model for the simulation of EG uses the dipole–dipole interaction approach introduced by Devarajan and Glazer [8] as a principal point, which evaluates the optical rotation and the refractive indices.

In a static field the polarization is caused by a shift of the nucleus in the direction of the electric field vector. However, this model is limited to structures with small polarizability [9], to which chiral-like materials belong. In this case the occurrence of screw-like polarization using a conception of rotational circular oscillators (or so-called gyrooscillators) [10, 11] seems to be more appropriate. Unfortunately, they are non-stable against the laser treatment which is necessary for the creation of the induced helicoidal-like grating due to relatively large molecular reorientation. From this point of view the use of inorganic NCs and particularly nanocomposites (nanocrystallites incorporated within sol–gel matrices), seems to be more appropriate.

Moreover, the NCs themselves create additional nanoconfined levels and the rare-earth ions cause additional polarization-enhancing effects of the space dispersion determined by the a/λ ratio [12], where a is the size of the NC and λ is the optical wavelength.

Recently a possible new way to enhance the role of internal axial symmetry was proposed [13, 14]. However, its technical realization is not possible at the moment.

In this work we use optical poling by circularly polarized light as a generator of the helicoidal-like structure. The general principles of optical poling were proposed and realized in different disordered materials, and particularly in glasses [15], however for linearly polarized light. The basic principle of optical poling consists in the creation of an acentric $\chi^{(2)}$ grating in the initially disordered materials during the interaction of two coherent bicolour beams with different intensities originating from the same laser source. In this case one can observe optical second harmonic generation described by third-rank polar tensors. In order to enhance the EG effect in the nanocomposites following general consideration one can use similar optical poling, but using circularly polarized interacting bicolour coherent beams. In this case the optically induced effect will be a superposition of the nanoconfined exciton contribution and the photostimulated axial grating polarization.

So the EG effect described by an axially symmetric third-rank tensor should be substantially enhanced in this case. As an effect of the space dispersion [12] it requires the existence of a sufficiently large ratio of a/λ and high density of the localized nanoconfined and f-electron states.

Using the idea of self-organization for the transition dipole moments proposed by Antonyuk [16], one can extend it for the NCs incorporated into the glass matrix. Recently, the crucial role of the photoinduced quasi-phonons was also demonstrated [13], substantially rescaling the optical parametrical phenomena. The photoinduced axially symmetric piezoelectric and electrostricted quasi-phonons may be extremely crucial for NCs doped by rare earths.

Among the semiconductor NC materials one of the more promising seems to be gallium nitride. Recently photoinduced non-linear optical effects were also observed in these nanocrystallites [17].

Gallium nitride, GaN, is a semiconductor material with energy gap equal to about $E_g = 3.4$ eV at room temperature. It has many applications in optoelectronic devices and biosensors, such as light-emitting diodes (LEDs), laser diodes (LDs) and detectors. The recent discovery of the special monochromatic luminescence properties of GaN doped with rare earths (REs) can lead to new types of light-emitting devices. Rare-earth-doped semiconductors have been of particular interest due to their unique optical and electrical properties. Their RE luminescence at ambient temperature only insignificantly depends on the nature of the host. All the mentioned properties allow us to consider GaN nanocrystallites as more promising materials for multi-functional optoelectronic devices.

In the present work we will explore circularly-light-induced EG and associated axially symmetric second-order optical effects in Eu^{3+} - and Tb^{3+} -doped GaN nanocrystallites incorporated into a silica xerogel glass matrix.

2. Experimental details

2.1. Sample preparation

Portions of 0.355 g Eu_2O_3 and 0.383 g Tb_4O_7 were separately solubilized in hot concentrated nitric acid and were evaporated to dryness. Each of the residues was dissolved in 5 ml of distilled water acidified with HNO_3 to pH equal to 2 and added to a solution of 2.983 g $\text{Ga}(\text{NO}_3)_3 \cdot 9\text{H}_2\text{O}$ in distilled water (10 ml each). Finally, each of them was poured into 15 ml of tetramethoxysilane (TMOS) and vigorously stirred at room temperature for about 20 min.

The sol, tightly closed in a high density polyethylene container, was held for two weeks at room temperature. The applied preparation method was similar to that described by us earlier [18, 19]. When the gelation process was complete, the obtained gel was carefully dried in an oven, gradually increasing the temperature from 70 to 200 °C. Then, the xerogel was placed in an alumina crucible which was calcined at 500 °C for two days in open air to convert $\text{Ga}(\text{NO}_3)_3$ into Ga_2O_3 . The crushed gel sample was placed at room temperature into a quartz tube (24 mm ID) in flowing NH_3 ($120 \text{ cm}^3 \text{ min}^{-1}$), and after purging (20 min) the sample was heated ($5 \text{ }^\circ\text{C min}^{-1}$) to the required temperature of 750 °C and then was held for 15 h. The NH_3 used for nitridation (from Messer, Poland, 99.85 vol%) was additionally purified by passing it over a zeolite trap.

2.2. Structural features

The overall phase compositions of the nanopowders after each step of preparation were checked by x-ray powder diffraction with a Siemens D5000 diffractometer and $\text{Cu K}\alpha 1$ radiation, $\lambda = 0.15406$ nm.

The microstructure and phase composition of the samples were studied by transmission electron microscopy (TEM), high-resolution transmission electron microscopy (HRTEM) and

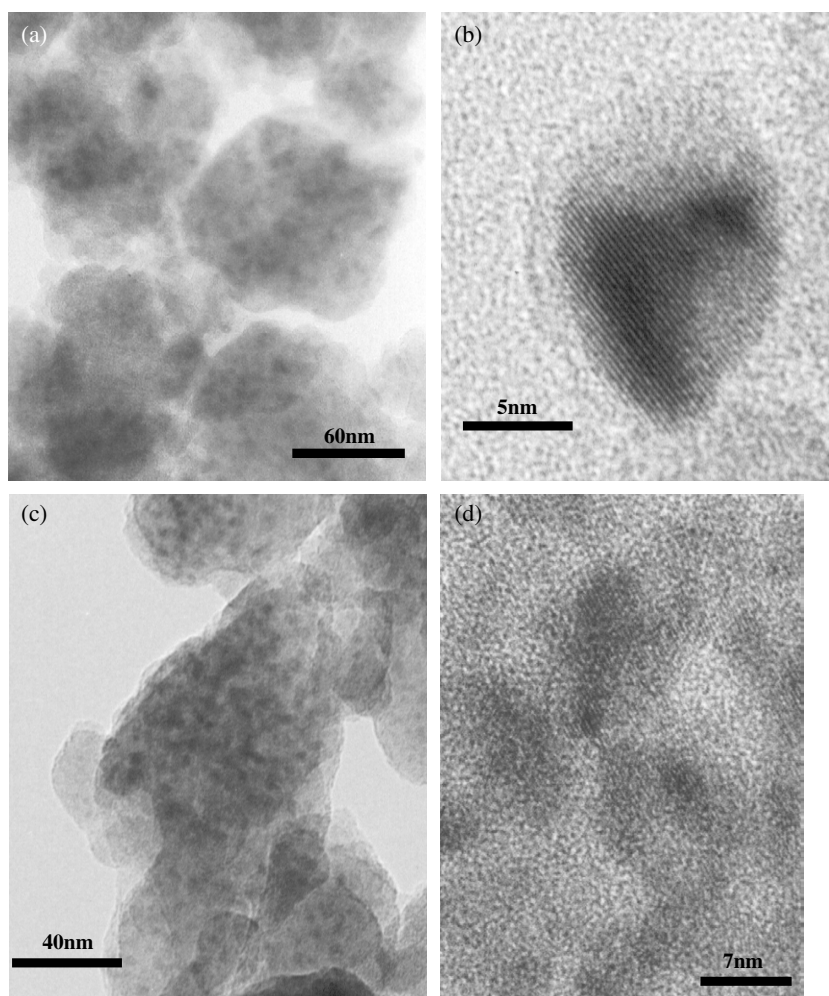


Figure 1. Typical TEM pictures of the GaN rare-earth-doped nanocrystallites: (a) and (b)—doped by Eu^{3+} ; (c) and (d)—doped by Tb^{3+} .

selected area electron diffraction (SAED) with a Philips CM 20 electron microscope operated at 200 kV and providing 0.24 nm point to point resolution. Specimens for the TEM studies were prepared by ultrasonically dispersing the sample in methanol, and depositing a droplet onto a copper microscope grid covered with a holey carbon film.

The XRD spectra (not show here) of calcined and nitrated composites did not show diffraction peaks which could be ascribed to gallium oxide or nitride formation. This could be due to the extremely high dispersion and small sizes of gallium oxide or gallium nitride particles.

The TEM inspection of nitrated samples revealed the presence of GaN NCs uniformly distributed in the matrix of both samples (cf figures 1(a) and (c)). High-resolution images (figures 1(b) and (d)) show lattice fringes of 2.79 and 2.55 Å, respectively, which could be ascribed to the nanocrystals of GaN. The mean particle sizes of GaN seem not to exceed 10 nm. The formation of the separate phases of europium or terbium oxides or their nitrides was not confirmed with the TEM method.

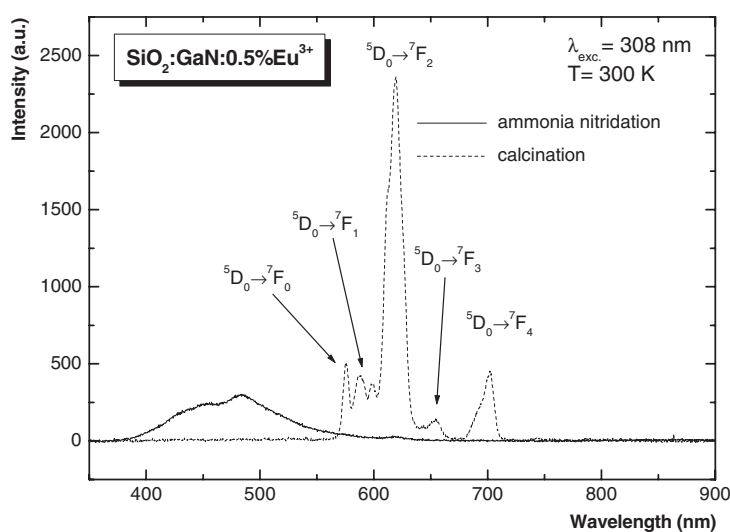


Figure 2. Photoluminescence spectra of $\text{SiO}_2:\text{GaN}:\text{Eu}^{2+,3+}$ samples: calcined and nitrided.

2.3. EPR and photoluminescence parameters

The electron paramagnetic resonance experiments were performed using a standard X-band EPR spectrometer equipped with an Oxford gas flow cryostat.

Photoluminescence (PL) spectra were measured using a Jobin–Yvon TRW 1000 spectrophotometer and a Hamamatsu R928 photomultiplier. A Lambda Physics excimer laser was used as the excitation source ($\lambda_{\text{exc}} = 308 \text{ nm}$) for recording the PL spectra. Room-temperature cathodoluminescence (CL) spectra were measured with an Ocean Optics Spectrometer SD2000 with resolution of 0.3 nm mm^{-1} . The CL spectra were excited in vacuum ($<10^{-6} \text{ Torr}$) in the column of a Tesla transmission electron microscope operating at 60 and 90 kV with current beam ranging from 10 to $120 \mu\text{A}$. The emitted light was collected directly above the sample into an optical fibre bundle placed in the microscope column and leading to the spectrometer.

Figure 2 shows a typical PL spectrum of $\text{SiO}_2:\text{GaN}$ doped by 0.5 (at.%) Eu^{3+} before and after nitridation in flowing NH_3 for 15 h at 750°C . For the non-nitrided sample we observed typical spectra peaks which can be assigned to the $4f-4f$ core level transitions of Eu^{3+} . After nitridation only a blue luminescence band centred at about 470 nm, probably due to the change of the oxidation state of the europium ion, is registered. This result suggests that at least a part of Eu^{3+} ions is reduced to Eu^{2+} . Hreniak *et al* [20] also reported broad band emission with a maximum at 445 nm for an Eu and Al-doped silica glass heated at 1250°C , which was ascribed to the Eu^{2+} emission.

Figure 3 shows an EPR spectrum measurement at 6 K for the $\text{SiO}_2:\text{GaN}:\text{Eu}^{2+}$ glass (a) before ammonia nitridation, compared to the EPR spectrum of $\text{SiO}_2:\text{GaN}:\text{Eu}^{2+}$ (b) after ammonia nitridation. The broad featureless absorption at $g \sim 2.05$ in the EPR spectra corresponds to ion–ion interaction. We have observed growth of the Eu^{2+} ion concentration after ammonia nitridation. Generally, the concentration of Eu^{2+} ions is a function of the area under the absorption curve [21]. In the development of rare-earth-doped laser glasses, great efforts had been devoted to avoid concentration quenching, resulting from an aggregation (or a chemical clustering) of the rare-earth oxide. Hayakawa *et al* [22] recorded the EPR spectra

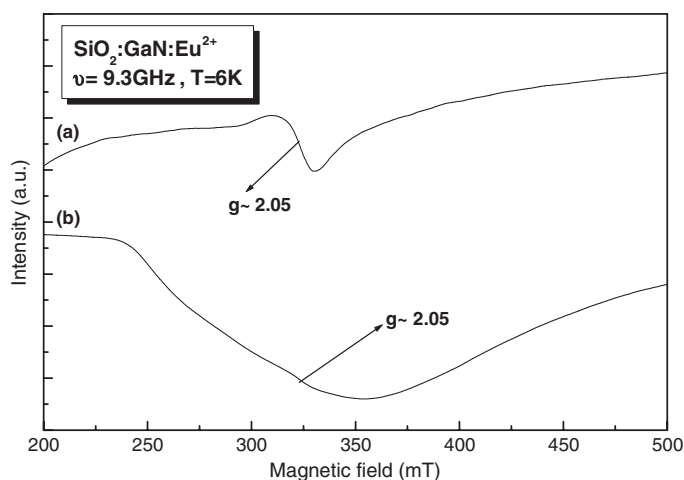


Figure 3. Electron paramagnetic resonance spectra for (a) $\text{SiO}_2\text{:GaN:Eu}^{2+}$ glass after calcination and (b) $\text{SiO}_2\text{:GaN:Eu}$ glass after ammonia nitridation.

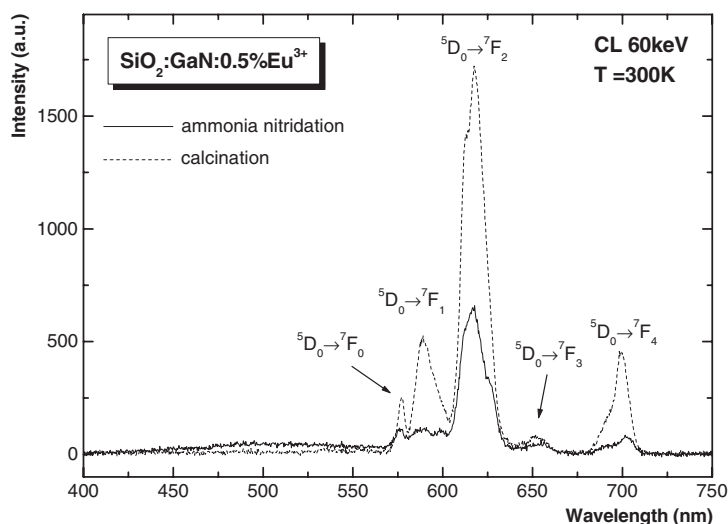


Figure 4. Cathodoluminescence spectra of $\text{SiO}_2\text{:GaN:Eu}$ samples: calcined and nitrided.

of Eu^{2+} -doped $\text{Al}_2\text{O}_3\text{-SiO}_2$ and SiO_2 glasses demonstrating a broad feature at $g \sim 2.0$. The broadening width for both of the paramagnetic glasses is nearly the same. They suggested that this broadening should be ascribed to a multi-site distribution of divalent europium ions. In our results the observed CL (see figure 4) is due to the ${}^5\text{D}_0 \rightarrow {}^7\text{F}_J$ ($J = 0, 1, 2, 3, 4$) of Eu^{3+} in SiO_2/GaN . A weak blue band emission of Eu^{2+} was also observed. The excitation processes of RE ions can generally be divided into two categories: direct and indirect excitation processes. The direct excitation process occurs by selective excitation of $4f^n$ electrons.

The PL and CL spectra of $\text{Tb}^{3+}\text{:GaN-SiO}_2$ composites measured at room temperature are shown in figures 5(a) and (b). The ${}^5\text{D}_4 \rightarrow {}^7\text{F}_J$ ($J = 6, 5, 4, 3$) transitions are assigned for the Tb^{3+} ions. Detailed studies of the luminescence properties of the undoped $\text{SiO}_2\text{:GaN}$ composites were presented in our previous paper [18].

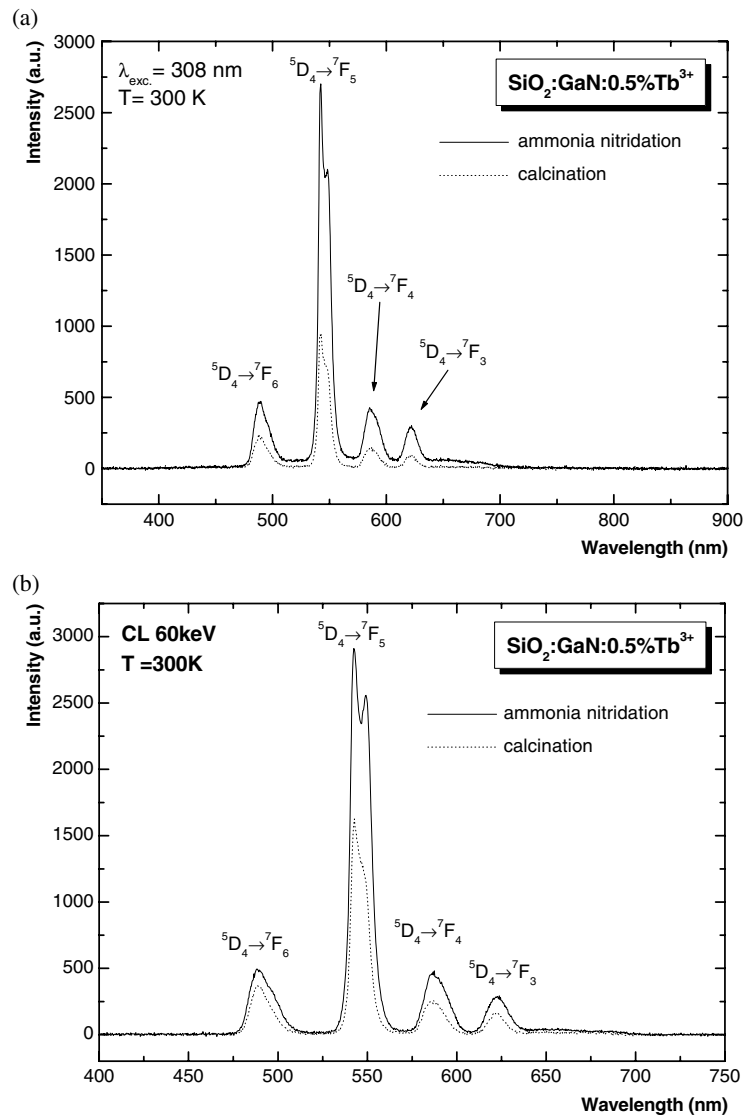


Figure 5. (a) Photoluminescence spectra of $\text{SiO}_2:\text{GaN}:\text{Tb}^{3+}$ samples: calcined and nitrided. (b) Cathodoluminescence spectra of $\text{SiO}_2:\text{GaN}:\text{Tb}^{3+}$ samples: calcined and nitrided.

3. Circularly light polarized electrogyration. Results and discussion

The principal set-up for the performance of the measurements is given in figure 6. As a probing beam a continuous GaAlAs semiconducting laser ($\lambda = 694 \text{ nm}$) was used with a power about 3.8 mW. For investigation of the EG the probing light beam was modulated by polarization using a Faraday modulator with a frequency of about 180 kHz. Using a traditional Senarmont scheme (figure 6) we evaluated the angle of the probe beam's rotation during application of the external electrostatic field perpendicularly to the probe beam propagation. The angle between the pump and probe beams did not exceed 8° . The system of polarizers P and mirrors M allowed us to achieve a good overlap between the pump and probe laser beams. From the

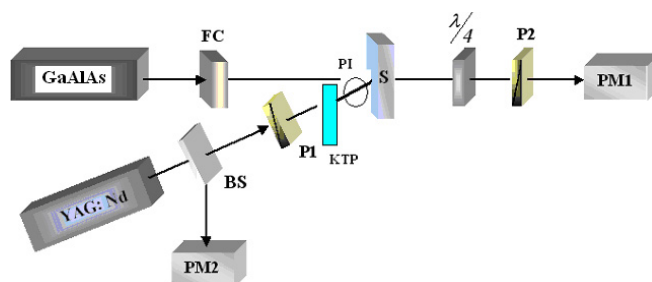


Figure 6. Experimental set-up for the measurements of the circularly polarized electrogyration. All the explanations are given in the text. FC—Faraday Cell; S—sample; BS—beamsplitter; PM—photomultipliers; $\lambda/4$ —phase plate; PI—phase inverter from the KDP for operating by circularly polarized light; KTP—single KTP crystals cut under phase-matching conditions. After the KTP crystal we have two coherent beams with fundamental and doubled frequency, the polarization of which is varied by the phase inverter PI.

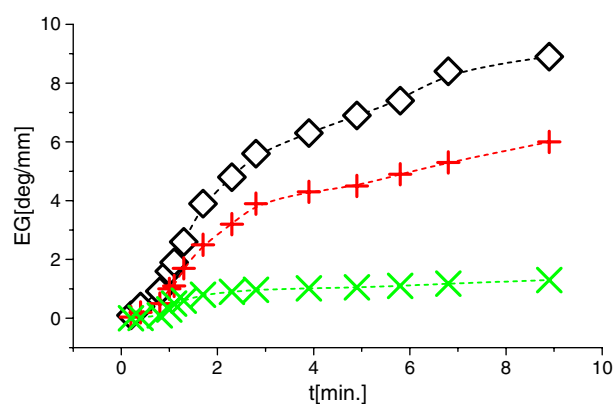


Figure 7. Variation of the electrogyration at temperature about 80 K for the different samples: \diamond —Eu-doped GaN; + —Tb-doped; \times —GaN-K500, 484.

pump Nd:YAG pulse laser ($\lambda = 1.06 \mu\text{m}$; pulse time duration 25 ps; optical power density up to 0.08 GW cm^{-2}) the beam was doubled in frequency using a crystal of KTP. Rotating the KTP crystal allowed to vary a ratio between intensities of fundamental and doubled-frequency beams.

The use of circularly polarized light for the creation of an axially symmetric medium opens a promising possibility for the observation of optically poled phenomena described by axially symmetric tensors of different orders. Among them the EG is of particular interest. We expect to create screw-like polarized medium.

From the above, it is clear that the use of GaN nanocrystals embedded within the very stable SiO_2 matrices may lead to an improvement of stability of the written helicoidal (screw-like) grating as well as to the enhancement of grating efficiency during the rare-earth doping.

The measurements were done during the optical treatment as well as after switching off the treatment.

The maximal increase of the output EG is observed during the first 10 min of circularly polarized optical treatment (preparation of helicoidal-like grating) (figure 7) at liquid helium temperature and applied electric field strength equal to about 350 V cm^{-1} . We have found that the maximal value of the EG is achieved for the Eu-doped NC, and it was equal to about

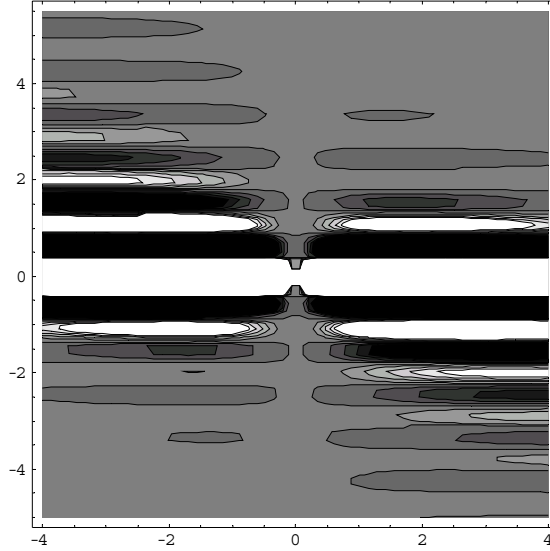


Figure 8. Typical profile of the optically treated GaN nanocomposites. The picture is obtained from cross-phase polarized microscopy.

$8.8^\circ \text{ mm}^{-1}$. The Tb-doped samples show lower effects, and pure GaN shows substantially lower output equal to about $5.4^\circ \text{ mm}^{-1}$ (see figure 7). It is necessary to emphasize that the effect was observed only at temperatures below 80 K. This may reflect a crucial role played by the trapping nanoconfined levels together with the polaron effects. Simultaneously the large polarizabilities caused by the rare-earth ions substantially contribute to the corresponding axially symmetric third-rank tensors.

Optically polarized measurements have shown that in our experiment the induced helicoidal-like grating has a complicated topological profile along the direction of the light propagation for the plane which is perpendicular to the direction of the propagation of the beam (see figure 8). The cross-section size of the induced grating is formed by the convolution of the cross-section distributions of incident radiations with the fundamental and the doubled frequency.

Such complicated topology may be explained within a framework of interaction of two coherent circularly polarized electromagnetic waves $\mathbf{E}_1(\omega) = \mathbf{e}_1 A_1(\mathbf{r}) \cos(\omega t + \mathbf{k}_1 \mathbf{r})$ and coherent second-harmonic $\mathbf{E}_2(2\omega) = \mathbf{e}_2 A_2(\mathbf{r}) \cos(2\omega t + \mathbf{k}_2 \mathbf{r})$ beams. The circularly induced poling process in this case is a result of their non-linear interaction $\omega + \omega - 2\omega \rightarrow 0$, leading to a non-zero coherent photocurrent possessing axial symmetry:

$$\mathbf{J} = \mathbf{e}_J A_1^2 A_2 \cos(\mathbf{q}\mathbf{r}) \quad (2)$$

and accumulation of the periodic electrostatic field \mathbf{E}_0 in accordance with the electrodynamic equations:

$$\frac{d\rho}{dt} = \text{div}(\mathbf{J} + \mathbf{J}_c), \quad \text{div}(\varepsilon \mathbf{E}_0) = -4\pi\rho. \quad (3)$$

The form of the $\mathbf{A}_0(\mathbf{r})$ depends on the spatial distribution of the interacting beams. It is obvious that when we have interaction of the incident axial Gaussian beams then the $\mathbf{A}_0(\mathbf{r})$ is formed by a simple convolution of the beams' cross-sections. In this case the induced charge density within the medium is a consequence of the superposition of different harmonics renormalized

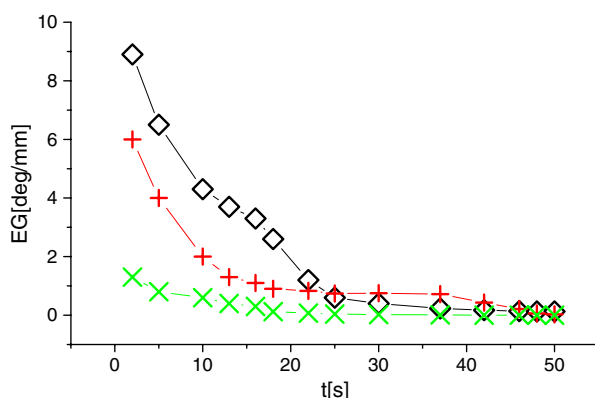


Figure 9. Relaxation time of the EG kinetics. The explanation of the samples is the same as in the figure 2.

by rotation of the medium (see figure 8). Transformation from circularly polarized to linearly polarized fundamental and writing beams suppresses the effect of the EG. Moreover, after switching off the external optical treatment the effect disappears during the first 15 s (see figure 9).

One of possible mechanisms explaining the observed long-lived helicoidal structure can be related to the occurrence of circular electrostricted phonons and diffusion processes effectively depopulating the appropriate trapping levels. The major role in the observed kinetics should play axial-like phonons created during interactions of the laser beams. The corresponding effect is an axially symmetric electrostricted effect described by a fourth-rank γ_{ijkl} tensor which is allowed by symmetry in the disordered media:

$$\sigma_{ij} = \gamma_{ijkl} E_k^{(0)} E_l^{(0)}. \quad (4)$$

The mechanical stress second-rank tensor γ_{ijkl} induces a phonon displacement field with effective vectors directed along the i and j directions. The considered phonons interact with the localized trapping states, changing their living times and polarizabilities substantially. In particular there occur long-lived polaron (autolocalized phonon) states causing an anisotropy of the diffusion coefficients D . The anomalous temperature behaviour of the EG versus the temperature (see figure 10) may serve as a confirmation of the specific role played by electron–phonon interaction.

During the illumination by circularly polarized light, the diffusion coefficient D of the bound electron–phonon (polaron) states decreases, stimulating additional polarization of the excited nanoconfined and localized rare-earth levels. The appearance of an additional number of trapping levels leads to the occurrence of a larger number of delocalized states within the forbidden energy gap. At the same time the polarizability caused by rare earths favours an additional enhancement of the effect. As a consequence we observe the relaxation of the EG after switching off the interacting coherent optical beams (figure 9).

4. Conclusion

During pumping of the GaN NCs by two circularly polarized bicolour coherent light beams with peak power density about 3.5 MW cm^{-2} it was found that there was an increase of the output EG during the first 10 min of circularly polarized optical treatment (preparation of helicoidal-like grating). We have clearly shown that the maximum of the EG is achieved for a fundamental to doubled frequency ratio of about 16 and after about 10 min of treatment.

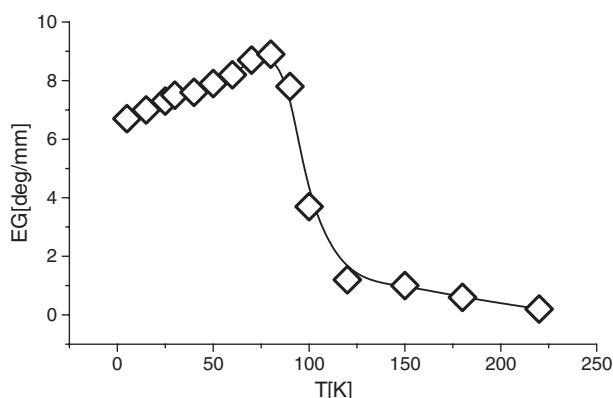


Figure 10. Temperature dependence of the EG at electric strength 350 V cm^{-1} , pump power density about 3.5 MW cm^{-2} .

We have found that the maximal value of the EG is achieved for the Eu-doped NCs, and it was equal to about $8.8^\circ \text{ mm}^{-1}$. The Tb-doped samples show lower effects (equal to about $5.4^\circ \text{ mm}^{-1}$). It is necessary to emphasize that the effect was observed only at temperatures below 80 K. The optically measured EG is principally a new effect in the nanocrystallites, and it opens a new possibility for a photoinduced non-linear optical grating.

Acknowledgments

One of the authors (M Nyk) is grateful for a scholarship obtained from the Centre of Advanced Materials and Nanotechnology of the Technical University of Wrocław. The authors are grateful to L Krajczyk for performing electron microscope experiments.

References

- [1] Zheludev I S 1964 *Crystallography* **9** 501
- [2] Vlokh O G 1970 *Ukr. J. Phys.* **15** 759
- [3] Vlokh O G, Lazko L A and Nesterenko V Ya 1972 *Crystallography* **17** 1248
- [4] Vlokh O G, Lazko L A and Zheludev I S 1975 *Crystallography* **20** 654
- [5] Uesu Y, Sonmachi H and Kobayashi J 1979 *Phys. Rev. Lett.* **42** 1427
- [6] Weber H-J 2000 *J. Phys.: Condens. Matter* **12** 1485
- [7] Vlokh R, Kostyrko M and Kruchkevych V 2001 *Ukr. J. Phys. Opt.* **2** 86
- [8] Devarajan V and Glazer A M 1986 *Acta Crystallogr. A* **42** 560
- [9] Kaminsky W 2000 *Rep. Prog. Phys.* **63** 1575–640
- [10] Brasselet S and Zyss J 1998 *J. Opt. Soc. Am. B* **15** 257
- [11] Crassous J and Kityk I V 2005 *J. Mod. Opt.* at press
- [12] Ginzburg V L and Agranowicz V M 1989 *Kristaloptics and Space Dispersion* (Moscow: Nauka)
- [13] Lemercier G, Andraud C, Kityk I V, Ebothe J and Robertson B 2004 *Chem. Phys. Lett.* **400** 19–22
- [14] Danel K, Ozha K and Kityk I V 2005 *Chem. Phys.* at press
- [15] Antonyuk B P, Novikova N N, Didenko N V and Aktsipterov O A 2001 *Phys. Lett. A* **287** 161
- [16] Antonyuk B P 2003 *Light-Driven Self-Organization* (New York: Nova Inc.)
- [17] Kityk I V, Gruhn W and Sahraoui B 2004 *Opt. Lasers Eng.* **41** 51–6
- [18] Nyk M, Jabłoński J M, Stręk W and Misiewicz J 2004 *Opt. Mater.* **26** 133
- [19] Yang Y, Tran C, Leppert V and Risbud S H 2000 *Mater. Lett.* **43** 240
- [20] Hreniak D, Jasiorski M, Maruszewski K, Kepinski L, Krajczyk L, Misiewicz J and Strek W 2002 *J. Non-Cryst. Solids* **298** p.146
- [21] Ramesh Kumar V, Narasimhulu K V, Gopal N O, Rao J L and Chakradhar R P S 2004 *Physica B* **348** 446
- [22] Hayakawa T and Nogami M 2000 *Solid State Commun.* **116** 77